Variability in error-based and reward-based human motor learning is associated with entorhinal volume

Anouk J. de Brouwer[1], Mohammad R. Rashid[2], J. Randall Flanagan[1,3], Jordan Poppenk[1,3], Jason P. Gallivan[1,3,4]

1 Centre for Neuroscience Studies, Queen's University, Kingston, ON, Canada
2 School of Computing, Queen's University, Kingston, ON, Canada
3 Department of Psychology, Queen's University, Kingston, ON, Canada
4 Department of Biomedical and Molecular Sciences, Queen's University, Kingston, ON, Canada

Corresponding author: Anouk J. de Brouwer (ajdebrouwer@gmail.com)

Abstract

Error-based and reward-based processes are critical for motor learning, and are thought to be mediated via distinct neural pathways. However, recent behavioral work in humans suggests that both learning processes are supported by cognitive strategies and that these contribute to individual differences in motor learning ability. While it has been speculated that medial temporal lobe regions may support this strategic component to learning, direct evidence is lacking. Here we first show that faster and more complete learning during error-based visuomotor adaptation is associated with better learning during reward-based shaping of reaching movements. This result suggests that strategic processes, linked to faster and better learning, drive individual differences in both error-based and reward-based motor learning. We then show that right entorhinal cortex volume was larger in good learning individuals—classified across both motor learning tasks—compared to their poorer learning counterparts. This suggests that strategic processes underlying both error- and reward-based learning are linked to neuroanatomical differences in entorhinal cortex.

Keywords: motor adaptation, visuomotor rotation, explicit learning, reinforcement, individual differences

Significance Statement

While it is widely appreciated that humans vary greatly in their motor learning abilities, little is known about the processes and neuroanatomical bases that underlie these differences. Here, using a data-driven approach, we show that individual variability in error-based and reward-based motor learning is tightly linked, and related to the use of cognitive strategies. We further show that structural differences in entorhinal cortex predict this intersubject variability in motor learning, with larger entorhinal volumes being associated with better overall error-based and reward-based learning. Together, these findings provide support for the notion that the ability to recruit strategic processes underlies intersubject variability in both error-based and reward-based learning, which itself may be linked to structural differences in medial temporal regions.

Introduction

The human brain's capacity to learn new motor commands is fundamental to almost all activities we engage in. Traditionally, such learning has been viewed as an implicit, procedural process of the motor system, with neural studies focusing on brain areas in the frontoparietal cortex, striatum or cerebellum (Doya, 2000; Lalazar and Vaadia, 2008; Taylor and Ivry, 2014). Only relatively recently have studies demonstrated that cognitive systems, including processes related to strategy use and memory, can bolster or interfere with aspects of motor learning (Mazzoni and Krakauer, 2006; Keisler and Shadmehr, 2010; Taylor and Ivry, 2011; Seidler et al., 2012; Holland et al., 2018). It has been speculated, but not yet shown, that regions in the medial temporal lobe (MTL) may contribute to this cognitive component to motor learning.

In error-based learning, the form of learning by which we refine and adjust our movements to changes in the body or the environment based on observable errors, the use of cognitive strategies (often termed the 'explicit' component) has been shown to drive large, rapid changes during early learning (Taylor and Ivry, 2011; Taylor et al., 2014). This is in contrast to the implicit process, which contributes to learning in parallel but in a nonconscious, gradual fashion. Whereas the reliance of the implicit process on the cerebellum is well established (Smith and Shadmehr, 2005; Tseng et al., 2007), the neural basis of the explicit component remains speculative. Evidence from neuroimaging, aging, and lesion studies have implicated areas in the prefrontal cortex in explicit strategies (Shadmehr and Holcomb, 1997; Della-Maggiore and McIntosh, 2005; Taylor and Ivry, 2014). In addition, it has been suggested that regions in the MTL, given their role

in declarative processes, may be involved in the explicit component to motor learning (Doyon and Benali, 2005; Taylor and Ivry, 2014; de Brouwer et al., 2018).

In reward-based learning, the form of learning in which motor commands are updated by signals related to success or failure (Sutton and Barto, 2018), the use of cognitive strategies have also been shown to play a pivotal role in performance (Codol et al., 2018; Holland et al., 2018). Conventionally, reward-based learning has been shown to involve neural circuits in the basal ganglia and striatum (Doya, 2000), but there is also some emerging evidence to suggest contributions from MTL regions (Gershman and Daw, 2017; Duncan et al., 2018). A key feature of reward-based learning is that it is achieved through exploration (i.e., the brain figuring out motor commands that increase success). Insofar as such exploration is facilitated by strategies, MTL structures may also contribute to performance during reward-based motor learning.

The role of MTL regions in declarative memory and spatial navigation have been well established (Eichenbaum and Cohen, 2014). In humans, for example, anatomical imaging methods have demonstrated clear links between individual differences in hippocampus and/or entorhinal cortex volume with performance in memory and navigation tasks (Maguire et al., 2000; Rodrigue and Raz, 2004; Whiteman et al., 2016; Sherrill et al., 2018). It is increasingly recognized, however, that the hippocampal-entorhinal system can support more abstract relational representations (Tavares et al., 2015; Constantinescu et al., 2016; Horner et al., 2016; Aronov et al., 2017), and forms a ‘cognitive’ map for representing goals and relating objects and actions within a spatial context (Tolman, 1948; O’Keefe and Nadel, 1978). Such maps are likely to be critical when forming new action-outcome associations, as is the case when searching for and implementing strategies during motor learning.

Here we asked whether individual differences in motor learning performance are linked to hippocampal and entorhinal volume in humans. To examine this, we had human participants undergo a structural neuroimaging session in addition to performing separate error-based and reward-based learning tasks, both known to elicit the use of strategies. We show that learning performance in both motor tasks is directly related and that better overall learning across tasks is associated with larger entorhinal cortex volume.

Materials and Methods

Participants

The current study used a subset of participants (N=34; 18 men and 16 women, aged 20-35 years) from a larger cohort study (registered at https://osf.io/y8649) in which 66 right-handed paid volunteers underwent structural and resting state MRI scans. Our thirty-four participants took part in an error-based and reward-based motor learning testing session in addition to participation in the main study. One of these participants was excluded from further analysis because of a high number of invalid trials in the error-based learning task (>25%), thus leaving 33 participants for analysis.

The main experiment and motor learning follow-up tasks were approved by the Queen's University Health Sciences Research Ethics Board, and participants provided written informed consent before participating in the main experiment and in the motor learning session. The motor learning session took approximately an hour and 45 minutes and participants were compensated $20 for their time. The methods, hypotheses and data analyses for the current study were pre-registered on OSF (https://osf.io/7prq5).

Neuroimaging

Procedure

The day prior to each participants' MRI scan, participants completed a biofeedback session in a simulated (mock) MRI scanner to become familiar with the MRI environment and to learn to minimize head movement. During the biofeedback session, participants viewed a 45-minute documentary with a live readout trace of their head motion overlaid. When their head motion exceeded an adaptive threshold, the documentary was paused for several seconds while static was played on the screen along with a loud, unpleasant noise. The next day, MRI data were collected over the course of a 1.5-hour session using a 3T whole-body MRI scanner (Magnetom Tim Trio; Siemens Healthcare). We gathered high-resolution whole-brain T1-weighted (repetition time [TR] 2400 ms; echo time [TE] 2.13 ms; flip angle 8°; echo spacing 6.5 ms) and T2-weighted (TR 3200 ms; TE 567 ms; variable flip angle; echo spacing 3.74 ms) anatomical images (in-plane resolution 0.7 × 0.7 mm_2; 320 × 320 matrix; slice thickness 0.7 mm; 256 AC-PC transverse slices; anterior-to-posterior encoding; 2 × acceleration factor) and an ultra-high resolution T2-weighted

volume centred on the medial temporal lobes (resolution 0.5 x 0.5 mm_2; 384 × 384 matrix; slice thickness 0.5 mm; 104 transverse slices acquired parallel to the hippocampus long axis; anterior-to-posterior encoding; 2 x acceleration factor; TR 3200 ms; TE 351 ms; variable flip angle; echo spacing 5.12 ms). The whole brain protocols were selected on the basis of protocol optimizations designed by Sortiropoulos and colleagues (2013). The hippocampal protocols were modeled after Chadwick and colleagues (2014). In addition, we acquired two sets (right-left direction and left-right direction) of whole-brain diffusion-weighted volumes (64 directions, b = 1200 s/mm_2, 93 slices, voxel size = 1.5 × 1.5 × 1.5 mm_3, TR 5.18 s, TE 103.4 ms; 3 times multiband acceleration), plus two extra B0 scans gathered separately for each orientation.

Data analysis

Automated cortical and subcortical segmentation of the T1-weighted and T2-weighted brain data was performed in Freesurfer (v6.0) (Fischl et al., 2002, 2004). For each hemisphere, we obtained the volume of the hippocampus (HC) and entorhinal cortex (EC) in the MTL for our main analysis. We also obtained striatal volumes, including left and right globus pallidus, putamen, caudate and accumbens for exploratory analyses (see *Supplemental Information*). Segmentations of these areas were checked visually and manually adjusted if necessary.

In addition to the Freesurfer segmentations, we obtained separate volumetric measures of the anterior and posterior hippocampus in each hemisphere. The ultra-high-resolution T2-weighted 0.5mm isotropic medial temporal lobe scans were submitted to automated segmentation using HIPS, an algorithm previously validated to human raters specialized in segmenting detailed neuroanatomical scans of the hippocampus (Romero et al., 2017). Three independent raters were trained on segmenting the hippocampus at the uncal apex into aHC and pHC segments, and achieved a Dice coefficient of absolute agreement of 80%. Two of these raters independently segmented all participants using the 0.5 mm T1-weighted scans. The T2-weighted medial temporal lobe scans were registered to the T2-weighted whole-brain scans, which were in turn registered to the T1-weighted whole-brain scans, and the combined transform was used to place the rater landmarks on the detailed medial temporal lobe scans. Finally, the total number of voxels in each subregion was multiplied by the volume of each voxel to obtain a total aHC and pHC volume.

To account for differences in head size, all regional volumes were corrected for total intracranial (IC) volume obtained from Freesurfer. This was done by first estimating the slope *b* of the

regression line of each regional volume on the IC volume across the 33 participants included in the analysis. Next, each regional volume was adjusted for the IC volume as: adjusted volume = raw volume - $b \times$ (IC volume - mean IC volume).

Motor learning tasks

General procedure

Thirty-four participants performed an error-based and a reward-based motor learning task. We attempted to fully counterbalance the tasks across participants; The first 19 participants performed the error-based motor learning task before performing the reward-based motor learning task, with the next 15 participants performing the reward-based motor learning task before the error-based motor learning task. The reward-based task took about 25 minutes to complete and the error-based task took about 65 minutes to complete.

Setup

Participants were seated at a table, with their chin and forehead supported by a headrest placed ~50 cm in front of a vertical LCD monitor (display size 47.5 × 26.5 cm; resolution 1920 × 1080 pixels) on which the stimuli were presented (Fig. 1A). Participants performed reaching movements by sliding a stylus across a digital drawing tablet (active area 311 x 216 mm; Wacom Intuous) placed on the table in front of the participant. Movement trajectories were sampled at 100 Hz by the digitizing tablet. Vision of the hand and tablet was occluded by a piece of black cardboard attached to the headrest. In the error-based learning task, eye movements were tracked at 500 Hz using a video-based eye tracker (Eyelink 1000; SR Research) placed beneath the monitor. The eye movement data were not analyzed in this study. The stimuli and motor learning tasks are described in detail below.

Reward-based motor learning

Task

Our task was inspired by the reward-based learning task designed by Dam and colleagues (Dam et al., 2013). Participants performed reaching movements from a start position to a target line by sliding the stylus across the tablet. They were instructed to “find an invisible curved path by drawing paths on the tablet and evaluating your score for each attempt”. Participants started with a practice block of 10 trials, in which they traced a visible, straight line between the start position

and the target, to become familiar with the task and the timing requirement of performing the movement within 2 s. Next, participants performed 12 blocks, each containing 20 attempts to copy an invisible path, which differed in each block.

Each trial started with the presentation of a start position (5 mm radius circle; Fig. 1B). After the participant had moved the cursor to the start position and held it there for 200 ms, a horizontal target line (30 x 1 mm) would appear 15 cm in front of the start position, and a rectangular outlined box (320 x 170 mm) would appear around the start position and target. Next, participants drew a path from the start position to the target line while remaining in the box. After crossing the target line, the cursor disappeared, and a score between 0 and 100 was displayed centrally (for 1 s), indicating how close they were to the invisible path. Following this, all stimuli disappeared, and a new trial would start with the presentation of the start position and the reappearance of the cursor. If the movement duration was longer than 2 s, the score was not presented and the trial was repeated.

The invisible paths consisted of single curves (i.e., half sine waves; 6 blocks) and double curves (i.e., full sine waves; 6 blocks) of different amplitudes (± 0.2, 0.5 and 0.8 times the target distance; see inset of Fig. 1C), drawn between the start position and the center of the target line. Participants were not informed about the possible shapes of the invisible lines. The trial score was computed by taking the x position of the cursor at every cm travelled in the y-direction (i.e., 1, 2, 3, … and 15 cm), and computing the absolute difference in x position between the cursor and the invisible line at the corresponding y-distance. The sum of these errors was then normalized by dividing it by the sum of distances between a straight line and a curve with an amplitude of 0.5 times the target distance, and multiplied by 100 to obtain a score between 0 and 100 (negative scores were presented as 0).

All participants performed one practice block and 12 experimental blocks of trials. Ten different randomized orders of experimental blocks were created. Participant 1, 11, 21, and 31 performed the first order, participant 2, 12, 22, and 32 performed the second order, etc.

Data analysis

The median score in trials 11 to 20 of each block of 20 attempts were used as a measure of learning performance. We did not use trials 1-10 in our analysis based on our frequent observation that participants who learned fairly quickly often used exploratory strategies when encountering

a new path, which often resulted in scores of, or around, zero on several trials (Fig. 2A provides a good example of such a participant). For each participant, we averaged the median scores across all single curves and across all double curves with the same amplitude. This resulted in two scores per participant.

Error-based motor learning

Task

Participants performed center-out reaching movements from a start position to one of eight visual targets presented on a 10 cm radius ring around the start position. Participants were instructed to hit the target with their cursor by making a fast reaching movement on the tablet, 'slicing' through the target. The ratio between movement of the tip of the stylus and movement of the cursor presented on the screen was 1:2, so that a movement of 5 cm on the tablet corresponded to a movement of 10 cm of the cursor. Participants first performed a baseline block in which they received veridical feedback about the position of the tip of the stylus, shown as a cursor on the screen. After performing a baseline block, participants performed a visuomotor rotation task, a task that has been used extensively to assess error-based learning (e.g., Cunningham, 1989; Krakauer et al., 2005). In this task, the movement of the cursor representing the hand position is rotated about the hand start location, in this experiment by 45º clockwise, requiring that a counterclockwise adjustment of movement direction be learned.

Each trial started with the participant moving the stylus to a central start position (5 mm radius circle; Fig. 1D). When the (unseen) cursor was within 5 cm of the start position, a ring was presented around the start position to indicate the distance of the cursor, so that the participant had to reduce the size of the ring to move to the start position. The cursor (4 mm radius circle) appeared when the cursor 'touched' the start position (9 mm distance). After the cursor was held within the start position for 500 ms, the target (6 mm radius open circle) was presented on an (imaginary) 10 cm radius ring around the start position at one of eight locations, separated by 45º (i.e., 0, 45, 90, 135, 180, 225, 270 and 315º). In addition, 64 non-target 'landmarks' (3 mm radius outlined circles, spaced 5.625º apart) were presented, forming a 10 cm radius ring around the start position. After a 2 s delay, the target would 'fill in' (i.e., color red), providing the cue for the participant to perform a fast movement to the target. If the participant started the movement before the cue, or more than 1 s after the cue, the trial was aborted and a feedback message indicating "Too early" or "Too late" appeared on the screen, respectively. In correctly timed trials, the cursor

was visible during the movement to the ring and then became stationary for 1 s when it reached the ring, providing the participant with visual feedback of their endpoint error. When any part of the cursor overlapped with any part of the target, the target would color green to indicate a hit. If the duration of the movement was longer than 300 ms, a feedback message “Too slow” would appear on the screen.

In trials in the rotation block, the movement of the cursor was rotated by 45º clockwise around the start position. To assess the contribution of the explicit process of learning, participants performed several ‘reporting’ trials. These trials were performed at the end of the first rotation block to ensure that participants’ learning behavior would not be influenced, as the reporting procedure itself can increase the proportion of participants that implement a cognitive strategy (3). In reporting trials, participants were instructed to, before each reach movement, report the aiming direction of their hand for the cursor to hit the target. They did this by turning a knob with their left hand, to rotate a line on the screen, positioned between the start position and the ring, to align it with their strategic aimpoint. When satisfied with the direction of the line, the participant clicked a button positioned next to the knob, and the line disappeared. After a 1 s delay, the target filled in as a cue to execute the reach.

All participants performed 4 blocks of trials in total, where within each block, target locations were randomized within sets of eight: (1) A baseline block (5 sets of 8 trials; 40 in total), (2) a rotation block (10 sets of 8 trials without report + 2 sets of 8 reporting trials + 2 sets of 8 trials without report; 112 trials in total), (3) a washout block in which veridical cursor feedback was restored (10 + 10 sets with a 30 s break in between; 160 trials in total) and (4) a second rotation block to assess participants’ rates of re-learning (10 sets of 8 trials; 80 in total). Ten different randomized trial orders were created for the full experiment. Participant 1, 11, 21, and 31 performed the first order, participant 2, 12, 22, and 32 performed the second order, etc.

Data analysis

Trials in which the movement was initiated too early or too late (as detected online; 4% of trials) or in which the movement duration was longer than 300 ms (4% of trials), were discarded from the analysis. The median endpoint hand angle (i.e., the difference in angle between the target and the hand when the cursor crossed the ring) per set of eight trials was used as a measure of learning performance. To capture individual differences in the rate of early learning that correspond to the implementation of aiming strategies (Taylor et al., 2014; de Brouwer et al.,

2018), we computed, for each participant, early learning scores in the first and second rotation block. To do this, we averaged the median in sets 2 and 3 of each of these blocks (excluding the first set in which participants often showed highly variable behavior). To derive a direct measure of the magnitude of the explicit component of learning, we used the average of the median reported aiming angle with respect to the target, obtained in the reporting trials (sets 11 and 12 in the rotation block). This resulted in three measures per participant.

Relating learning measures and neuroanatomy

Data and statistical analysis

As a first exploratory step to determine relationships in subject performance across the error-based and reward-based learning tasks, we calculated Pearson correlations between the five learning scores across participants. Having identified patterns of covariation in subject-level performance across the two tasks, for our main analysis, we submitted the learning scores to a principal component analysis (PCA). This approach has three important advantages: (1) it identifies the main patterns of covariation both within and between tasks, (2) it reduces the number of behavioural variables to be used in further analyses, and (3) it provides us with uncorrelated measures of learning performance (i.e, principal components), suitable to use in linear regression. To do the PCA, we first transformed the variables from the error-based learning task, whereby all angles were converted to errors with respect to the target, such that zero corresponds to a target hit, negative errors (i.e., between -45º and 0º) correspond to no or partial compensation of the rotation, and positive errors correspond to overcompensation of the rotation. This transformation ensured that higher values on both the error-based and reward-based motor learning tasks were associated with better learning performance. We then standardized all scores before submitting them to the PCA. The principal components (PCs) were obtained using the pca function in Matlab, which uses a singular value decomposition algorithm to find PCs that capture the maximal variance in the data.

To test the hypothesis that better performance in the motor learning tasks is related to greater volumes of brain areas in the medial temporal lobe, we performed multiple linear regression analyses. All models were estimated using the fitlm function in Matlab, which returns a least-squares fit of the scores to the data. Our primary analysis included the left and right HC and EC volumes. To control for a potential effect of overall head size on learning performance, we also included each participant's total intracranial volume, making a total of five neuroanatomical

314 measures. For the first and second PC, we fitted a multiple linear regression model with the PC
315 as the dependent variable, and the set of four regional volumes plus the IC volume as predictors.
316 Previous studies have reported differential relationships between the anterior and posterior parts
317 of the hippocampus and memory (e.g., Maguire et al., 2000). Therefore, we performed a
318 secondary analysis, including the left and right anterior and posterior HC volume as predictors,
319 and the IC volume as a confounder.

320 ## Results

321 In order to determine the relationship between motor performance in reward-based and error-
322 based learning tasks, and the extent to which the size of hippocampal and entorhinal cortex may
323 be associated to such learning, we collected high-resolution structural MRI scans from
324 participants (N=34) prior to performing two separate motor learning tasks outside the scanner. In
325 the reward-based learning task, participants learned to copy an invisible, curved path through trial
326 and error, using only a score (between 0 and 100 points) to improve their performance. This score,
327 presented at the end of each trial, indicated how closely the participants' drawn path
328 corresponded to the invisible path (Fig. 1B). Participants drew these paths on a digital drawing
329 tablet from a start to a target position displayed on a vertical monitor (Fig. 1A), and were instructed
330 to maximize their score. To obtain a representative measure of each participant's reward-based
331 learning rate and ability, we had participants perform this task for 12 different invisible paths, with
332 20 attempts for each. Participants were naive to the possible shapes of the paths, which were
333 shaped as single curves (i.e., half sine waves) and double curves (i.e., full sine waves) between
334 the start and target position, with different amplitudes (see Fig. 1C). Because participants received
335 only visual feedback about their path trajectory—and never the rewarded path—they did not
336 receive error-based information that could be used to guide learning. By design, this reward-
337 based task requires implementing a search strategy to first find the invisible path and then refine
338 the drawn path, and we thus predict that participants who perform well in this task are better at
339 implementing such strategies.
340
341 For the error-based learning task, we used the classic visuomotor rotation learning paradigm
342 (Cunningham, 1989), wherein participants had to adjust their movements to a 45° rotation of the
343 cursor movement, which represented participants' hand movements, in order to hit visual targets
344 (Fig. 1D). Participants performed center-out reaching movements on the drawing tablet to one of
345 eight targets displayed on a monitor. After a baseline phase with veridical cursor feedback,

346 participants were exposed to the 45° visuomotor rotation of the movement of the cursor, requiring
347 an adjustment of the reaching movement in the opposite direction. Learning in this task consists
348 of two components: automatic, implicit adjustments of the reach direction, resulting in gradual
349 changes in performance, and the implementation of an aiming strategy to counteract the rotation,
350 resulting in fast changes in performance (Redding and Wallace, 1993; Taylor et al., 2014). Our
351 previous work has shown (de Brouwer et al., 2018) — and we predict here — that faster and more
352 complete learning is largely driven by the use of an aiming strategy, used to counteract the
353 rotation. At the end of the first block of rotation trials, we assessed this aiming strategy by asking
354 participants to report the intended aiming angle by turning a knob with their left hand to rotate a
355 line on the screen at the start of the trial, before executing the reach (Taylor et al., 2014). Learning
356 was then 'washed out' by restoring veridical cursor feedback, after which the visuomotor rotation
357 was re-instantiated to assess the rate of re-learning.

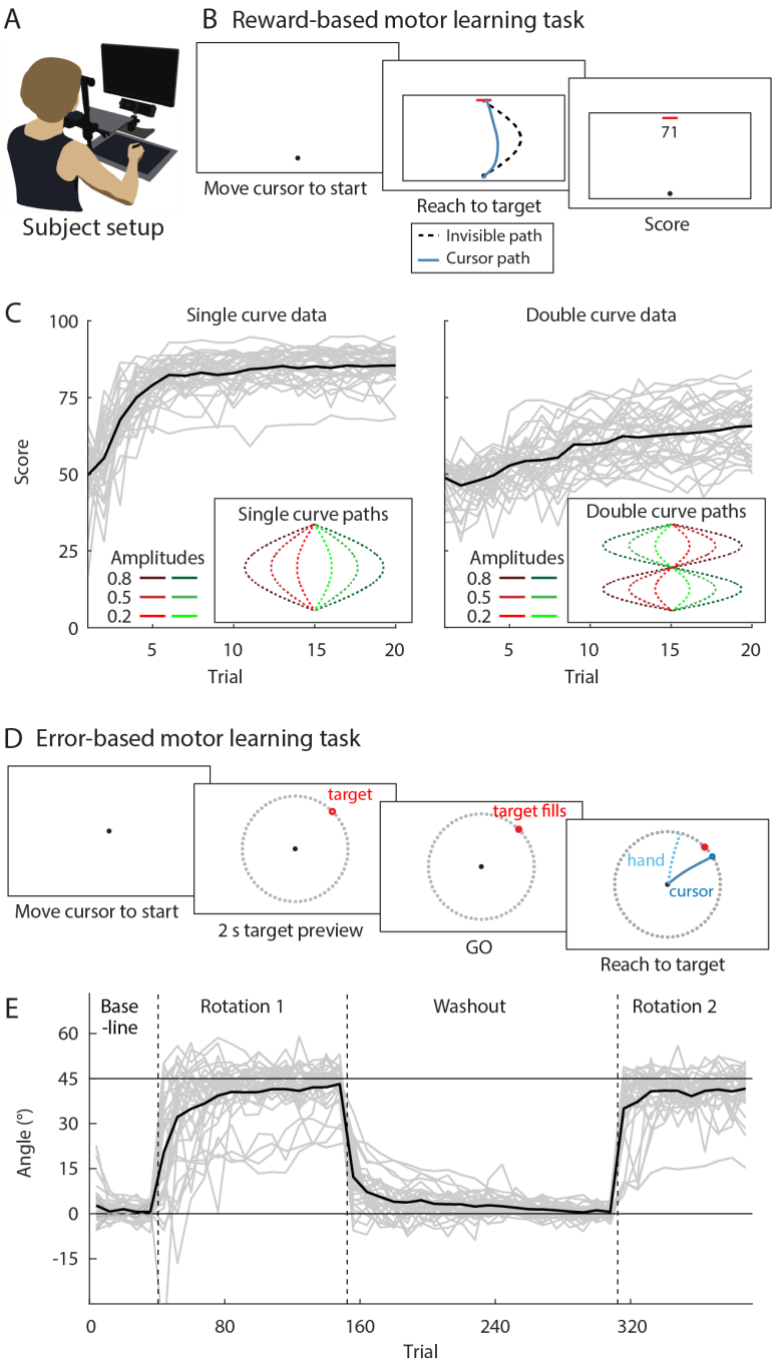

Figure 1. Experimental tasks and learning curves averaged across participants. (A) Setup. Participants made reaching movements by sliding a pen across a digitizing tablet without vision of the hand. The stimuli and a cursor representing the hand position were presented on a monitor. (B) Reward-based motor learning task. Participants were instructed to 'copy' an invisible path (dashed black line), with a score between 0 and 100 indicating how close their drawn path (blue line) was to the hidden path. (C) Learning across trials for single (left panel) and double invisible paths (right panel). Each grey line is an individual participant (n=33), with the black line representing the average across participants. Insets depict the six single curve invisible paths and the six double curve invisible paths used in the task. (D) Error-based motor learning task. Participants made center-out reaching movements to visual targets (red dot) on a ring of landmarks (small grey dots) with veridical cursor feedback (not shown) or under a 45° rotation of the cursor

feedback (blue line; hand direction is shown in light blue). (E) Learning curves (left panel) across the baseline, rotation 1, washout, and rotation 2 block. Each grey line represents an individual participant (n=33), the black line represents the mean across participants.

Performance in reward-based and error-based motor learning is related

The black traces in Figure 1C and 1E show the learning curves, averaged across all participants, for the reward-based and error-based learning tasks, respectively. These figures demonstrate that participants learned to increase their scores in the reward-based task and change their hand angle in the error-based task across trials. However, these group-averaged results may be somewhat misleading, as they obscure significant intersubject variability in both the rates and levels of learning obtained (see gray traces in Fig. 1C,E, which depict single participants). For example, Figure 2 shows the behavior of two participants, one 'good' overall learner and one 'poor' overall learner, in both the reward-based learning task and the error-based learning task. Figure 2A and 2B depict the paths that the participants drew (left panel) and the corresponding scores (right panel), in two blocks of the reward-based learning task for a single (top) and double curve (bottom) with the largest amplitude (blocks 4 and 11 for the participant in Fig. 2A; blocks 11 and 10 for the participant in Fig. 2B). While both participants quickly converged on a good solution for the single curve, resulting in scores close to 100, the movements of the participant in Figure 2A resemble the invisible curve more closely. In addition, while the participant in Figure 2A quickly converges upon a solution that has a similar shape to the invisible double curve, the participant in Figure 2B never learns to draw that same double curve, and their score remains low.

Figure 2C and 2D show, for the same two participants, the median hand angle (in blue) for each bin of eight trials across the error-based learning task, as well as the reported aiming angle (in purple) assessed near the end of the first rotation block. Appropriate corrections for the visuomotor rotation are plotted as positive values; that is, a hand angle of 45° corresponds to full compensation for the rotation. The participant in Figure 2C shows quick adjustment of the hand angle towards 45° in the first and second rotation block, and a quick return towards 0° in the washout block. Such fast learning is associated with a large contribution of an aiming strategy, consistent with their reported aiming angles around 39°. The participant in Figure 2D, by contrast, shows only gradual adjustments of the hand angle in the rotation and washout blocks, and correspondingly reports aiming values around 0°, suggesting that learning in this participant is mainly driven by the implicit process. Overall, the participant in Figure 2A,C showed better learning performance in both tasks than the participant in Figure 2B,D.

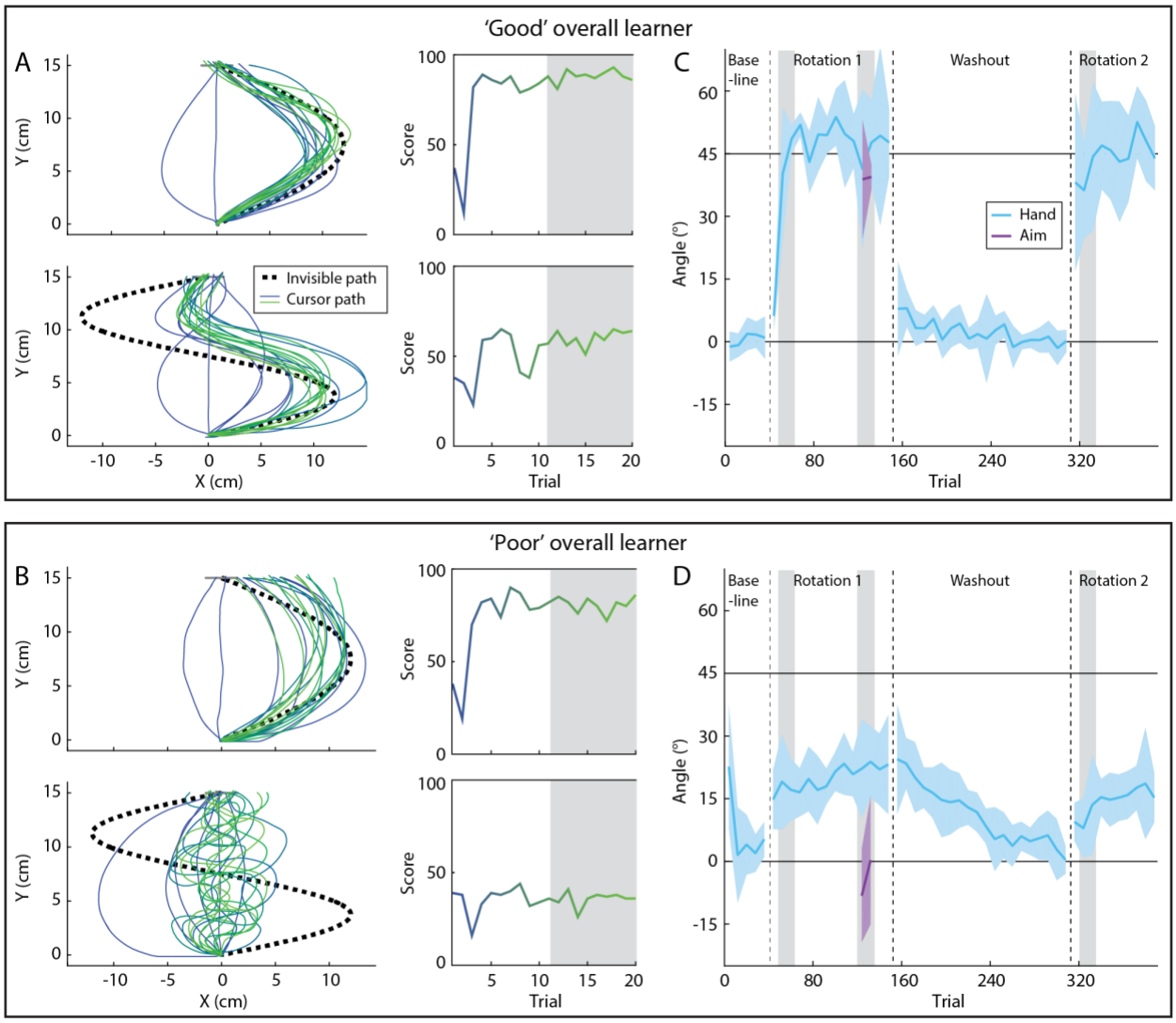

Figure 2. Example data of a 'good learner' and a 'poor learner'. (A,C) Data of an example 'good learner'. (A) Hidden path (dashed black line), drawn paths (blue and green lines), and score (blue to green gradient) for two blocks in the reward-based learning task. The median score in the last 10 trials of each block (grey shaded area) was used in further analyses. (C) Hand angle (light blue) and reported aiming angle (purple) relative to the target angle during the error-based learning task. Each data point represents the median of a set of eight trials, and the shading represents ± one standard deviation. The mean scores across sets 2 and 3 (early learning) of the rotation blocks were used in further analyses, as well as the averaged aiming angle (grey shaded areas). In the baseline and washout blocks, a hand angle of zero would result in a target hit, and in the rotation blocks, a hand angle of 45° results in perfect compensation of the rotated cursor path, and thus a target hit. (B,D) Same as (A,C), but for a 'poor learner'.

For each participant, we obtained two learning scores for the reward-based learning task (single and double curves) and three learning scores for the error-based learning task (early and late learning in rotation block 1 and 2, and the reported aiming angle; Fig 3A). Across the entire group of participants, we observed several significant correlations in the learning scores both within and

between the two tasks (Fig. 3B). Notably, the latter demonstrates clear patterns of covariation in subject-level performance across both the error-based and reward-based motor learning tasks. To derive single participant measures of learning that capture these patterns of covariation, and that can be used to relate overall learning performance to the neuroanatomical data collected in these same participants, we performed a principal component analysis (PCA) on the learning scores (see *Methods* for details). We found that the first (PC1) and second principal components (PC2) explained 53.8% and 22.3% of the variance in the data (76.1% overall), respectively. The projection plots in Figure 3C (left panel) allows for a straightforward interpretation of these PCs, directly showing both the magnitude and sign of the loading of each of our 5 learning measures onto PC1 and PC2. Notably, PC1 has positive loadings for all of the learning measures, indicating that this single component captures overall learning performance. Indeed, PC1 shows significant positive correlations with *all* behavioral learning measures from both tasks (ranging from r=0.55 to r=0.82, all p<0.001, see Fig. 3C, right panel). In other words, PC1 provides a single scalar measure that distinguishes between relatively 'good' versus 'poor' learning performance across *both* the reward-based and error-based learning tasks. The second principal component (PC2) broadly distinguishes between performance in the reward-based and error-based learning task, with positive loadings for the reward-based learning scores and negative loadings for learning in the rotation blocks. However, PC2 explains a relatively small portion of the overall behavioral variance (22.3%), limiting its interpretational value and its use in further analyses. Taken together, our dimensionality-reduction approach on the behavioral learning data demonstrates that subject-level performance in both tasks is highly related, as a single latent variable (PC1) captures whether participants are good learners in both the reward-based learning and in the error-based learning task.

Figure 3. Learning performance in the error-based and reward-based tasks is related and is captured by a single latent variable. (A) Distribution of scores for single and double curve performance in the reward-based learning task, and distribution of angular errors during early learning in the first and second rotation block, and reported aiming errors. Each dot indicates the mean value of one participant, the horizontal line indicates the mean across participants, and the shaded area indicates the standard error of the mean. (B) Scatterplots and associated Pearson correlations (uncorrected) within and between scores in the reward-based and error-based motor learning tasks across participants (n=33). This demonstrates subject-level covariation in learning performance both within and between the two tasks. (C) Principal component analysis loadings for the first and second principal component (PC) at left, and Pearson correlations between the first principal component and learning scores at right. This shows that PC1 provides a useful proxy for learning performance across both tasks. In (B) and (C), each dot represents one participant, and the black line represents the best fit regression line.

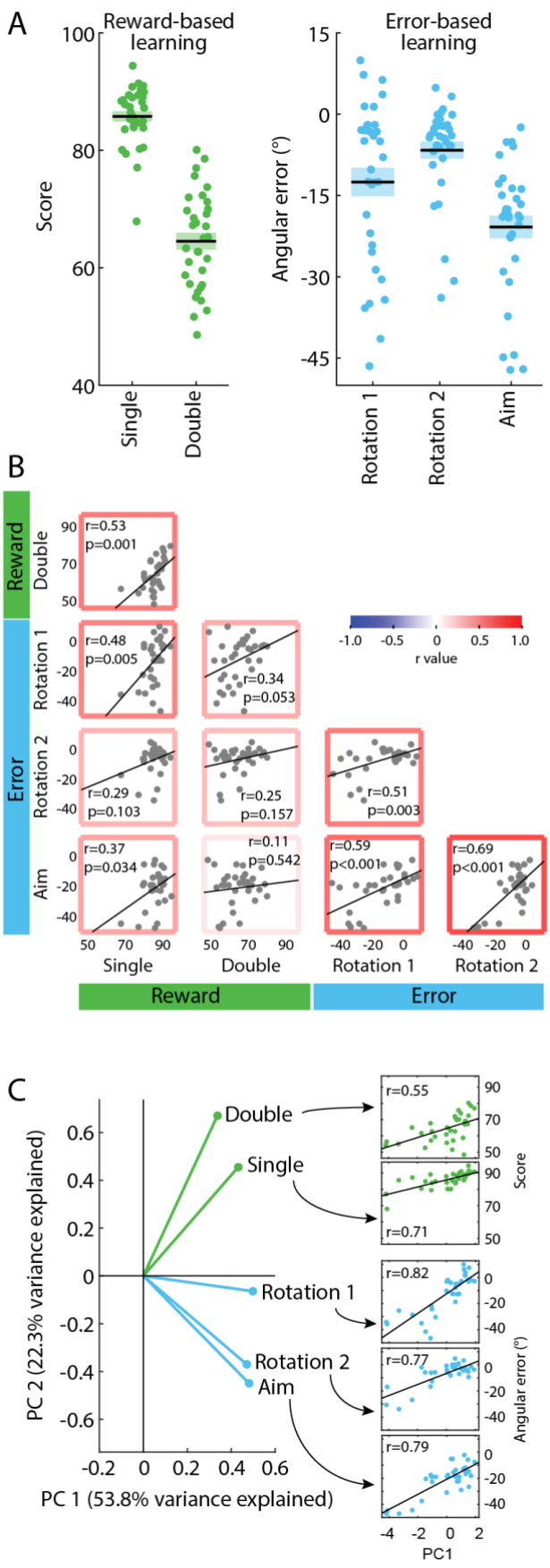

Larger entorhinal volume is associated with better error- and reward-based motor learning

Having clearly established that subject-level performance in reward-based and error-based learning is related and that this pattern of covariation can be captured by a single measure (i.e., PC1), our next aim was to determine whether this variation in performance is associated with the neuroanatomy of the MTL. To this end, we performed multiple linear regression analyses using right and left hippocampus (HC) and entorhinal cortex (EC) volumes as predictors and PC1 as the outcome variable (Fig. 4AB), corrected for total intracranial volume (see *Methods*). We also included total intracranial (IC) volume in our model to account for a potential effect of overall head size. Figure 4C shows the standardized regression coefficients and 95% confidence interval of the regression models for each PC. For PC1 — our measure of good vs. poor performance in both tasks — the model significantly explained the variance in PC1 score (model $F(5)=4.050$, $p=0.007$; $R_2=42.9\%$), with right EC volume being a significant predictor ($t=3.689$, $p=0.001$; see Figure 4-1). That is, larger right entorhinal volume corresponded with higher scores on PC1, or better overall learning in both tasks. Notably, we found no significant predictors of PC2 score (model $F(5)=0.410$, $p=0.806$, $R_2=7.1\%$), the measure that broadly distinguished between performance in the reward-based and error-based learning task. This lack of effect might not be surprising given that the percentage of variance in our motor learning data that was explained by the second principal component was fairly small (22.3%).

As a secondary analysis, we performed a linear regression with the anterior and posterior hippocampus as separate predictors, as previous studies have reported differential relationships between these individual parts of the hippocampus and memory (e.g., Maguire et al., 2000). However, here we again did not find significant relationships between left and right aHC and pHC volume and the score on PC1 (model $F(5)=0.360$, $p=0.871$, $R_2=6.2\%$) or PC2 ($F(5)=0.440$, $p=0.817$, $R_2=7.5\%$; Figure 4-2).

Taken together, the results of these regression analyses indicate that better performance in both reward-based and error-based learning is associated with larger right entorhinal volume.

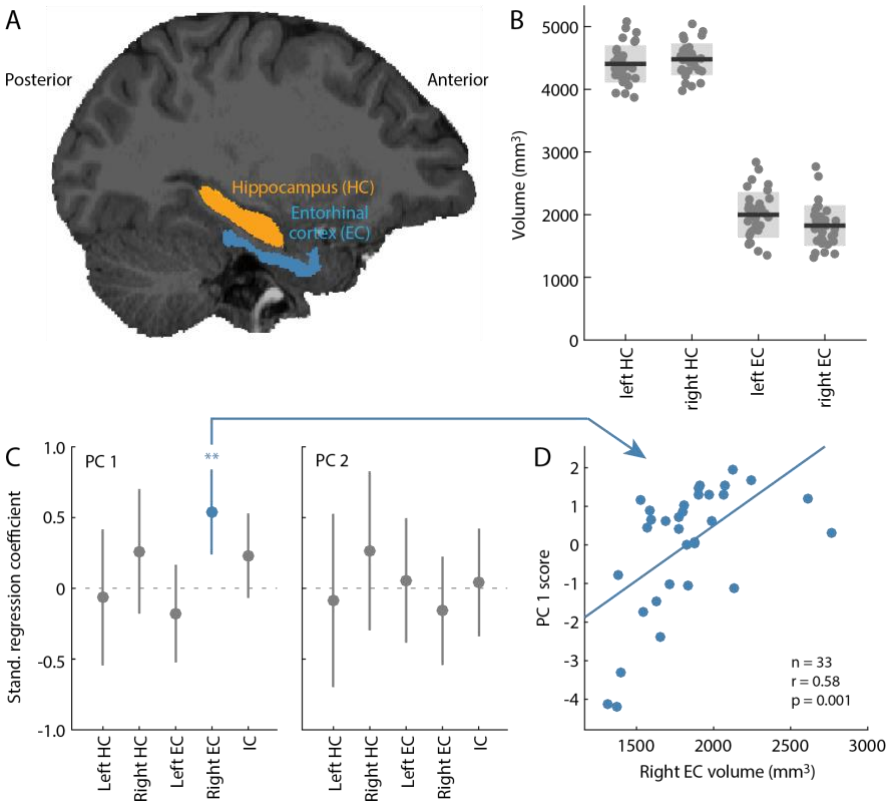

Figure 4. Larger entorhinal volumes are uniquely associated with better overall motor learning. (A) Illustration of the segmented hippocampus (orange) and entorhinal cortex (blue) in an example participant. (B) Volume of the left (L) and right (R) hippocampus (HC) and entorhinal cortex (EC), corrected for total intracranial volume (see *Methods*). Each dot depicts an individual participant (n=33), the dark grey line indicates the mean across participants, and the light grey area indicates the standard deviation. (C) Standardized regression coefficients and their corresponding 95% confidence intervals of the regression models to predict principal component 1 (PC 1; left panel) and principal component 2 (PC 2; right panel) based on the left and right hippocampus and entorhinal volumes, and the total intracranial volume (IC). See Figure 4-1 and 4-2 for all model coefficients and significance values. (D) Individual partial correlation between right entorhinal volume and PC 1 score. The line represents the best fit regression line.

Discussion

While previous work in motor learning has often studied error-based and reward-based learning processes in isolation from one another, recently there has been increased interest in understanding how these separate learning processes interact at the behavioral and neural levels. Here we find a strong relationship in intersubject variability between error-based and reward-based motor learning, showing that learning performance across tasks is correlated and can be explained by a single, latent variable. Our measures of learning and the nature of the tasks used suggest that this latent variable captures participants' use of cognitive strategies during learning, with higher scores on this variable being associated with faster and better overall learning in both

tasks. We further show, using structural neuroimaging and regression analyses with participants' hippocampus and entorhinal cortical volumes as predictors, that higher scores on this latent variable, and thus faster and better overall learning, is associated with larger right entorhinal cortex volumes. Together, these findings suggest that a shared strategic process underlies individual differences in error-based and reward-based motor learning, and that this process is associated with structural differences in entorhinal cortex.

Considerable computational and neural work has argued for a division of labor between the neural circuits that support error-based and reward-based learning (Doya, 1999, 2000; Daw and Doya, 2006; Shadmehr and Krakauer, 2008; Ito and Doya, 2011; Makino et al., 2016). According to this prevailing view, cortico-cerebellar pathways are responsible for error-based learning whereas cortico-striatal pathways are responsible for reward-based learning. Such distinctions, however, have often been reliant on indirect comparisons between different studies, and have been influenced by sampling biases in neural recording sites across different tasks. For instance, conventional views on error-based learning have suggested that adaptation is a primarily automatic mechanism, immune to reward-based feedback (Doya, 2000; Shadmehr and Krakauer, 2008). However, more recent behavioral evidence suggests that these two learning processes, while separable (Izawa and Shadmehr, 2011; Cashaback et al., 2017), interact during sensorimotor learning (Shmuelof et al., 2012; Taylor and Ivry, 2014; Galea et al., 2015; Nikooyan and Ahmed, 2015). Such interactions are likely to be supported by the recent demonstration of direct anatomical connections between the cerebellum and striatum (Bostan and Strick, 2018). These bidirectional connections could explain recent neural findings from rodents showing that the cerebellum, besides processing direction-related errors, also represents various aspects of reward-related information during task performance (Wagner et al., 2017; Heffley et al., 2018; Kostadinov et al., 2019; Larry et al., 2019). Together, this emerging evidence suggests that error-based and reward-based learning processes are closely intertwined at both the behavioral and neural levels.

There is also emerging evidence to suggest that both error-based and reward-based processes are mediated through the use of cognitive strategies implemented during learning. In error-based adaptation, the contribution of this explicit, declarative process to learning has been well-established behaviorally (Redding and Wallace, 1993; Fernandez-Ruiz et al., 2011; Taylor and Ivry, 2011; Taylor et al., 2014; Bond and Taylor, 2015; Haith et al., 2015; de Brouwer et al., 2018). Recent evidence from our group further indicates that faster learning across participants is linked

548 to individual differences in the magnitude of the cognitive strategy (de Brouwer et al., 2018), which
549 drives rapid changes early in the learning process. In reward-based learning, by contrast, the
550 contribution of cognitive strategies to performance have received comparably little attention, and
551 is only beginning to be established. As one example, recent work, wherein participants were only
552 provided with reward-based feedback (binary success/failure) to perform a visuomotor rotation
553 task, has shown that good versus poor learning is related to the implementation of a cognitive
554 component (Holland et al., 2018). This was evidenced by the observed reduction in reach angle
555 when participants were required to remove their aiming strategy (see also Codol et al., 2018). It
556 was also evidenced by the observation that the reward-based learning was impaired when (1)
557 participants had to perform a dual task (a separate mental rotation task) that divided their cognitive
558 load (Holland et al., 2018), or when (2) participants' reaction times were constrained (Codol et al.,
559 2018), such that they could not implement the strategy (Haith et al., 2015). To date, work
560 examining the link between error- and reward-based learning has focused on how reinforcement
561 signals (e.g., binary success/failure) shape learning in traditionally error-based tasks (Shmuelof
562 et al., 2012; Galea et al., 2015; Cashaback et al., 2017). By contrast, our current behavioral
563 findings show that, even when reward- and error-based learning is studied separately (and in very
564 different tasks), learning performance in both tasks is highly related — so much so that a single
565 latent variable can explain a significant proportion of intersubject variability in performance across
566 both types of learning.
567
568 Another novel result in our study was our finding that a larger right entorhinal volume was
569 associated with better overall learning in both the reward-based and error-based motor learning
570 tasks. The entorhinal cortex has been shown to support a wide range of cognitive functions that
571 would have bearing on various features of our motor learning tasks. Classically, the entorhinal
572 cortex, together with neighboring areas in the medial temporal lobe, has been implicated in spatial
573 navigation and memory through electrophysiological studies in rodents. These studies showed
574 that place cells in the hippocampus (O'Keefe and Dostrovsky, 1971) and grid cells in the
575 entorhinal cortex (Hafting et al., 2005) form a map-like representation of the environment. Grid
576 cells have also been demonstrated in primate entorhinal cortex, even in the absence of
577 locomotion, when the animal is simply exploring a visual scene with its eyes (Killian et al., 2012,
578 2015). Such observations have recently been extended to humans with functional MRI (Julian et
579 al., 2018; Nau et al., 2018), and there is even evidence suggesting that mere shifts in covert
580 attention (i.e., in the absence of overt eye movements), also elicits grid-cell-like responses in the
581 entorhinal cortex (Wilming et al., 2018). Together, these and other findings (Bellmund et al., 2016;

582 Constantinescu et al., 2016; Horner et al., 2016) have begun to reshape our understanding of the
583 role of the entorhinal cortex in visual-spatial memory, and in cognitive operations more generally.
584 An influential hypothesis is that the hippocampal-entorhinal system supports a cognitive map, an
585 idea that was originally proposed to explain findings in rodents (Tolman, 1948; O'Keefe and
586 Nadel, 1978) and later extended to humans (for review see Epstein et al., 2017). This hypothesis
587 proposes that the brain creates flexible representations of the environment to not only support
588 memory but also guide future decisions and effective (motor) behavior (Schiller et al., 2015;
589 Garvert et al., 2017; Bellmund et al., 2018).
590
591 In the context of the current study, we expect cognitive and spatial maps to be utilized during the
592 exploration of visuomotor space in our curve drawing (reward-based) and visuomotor rotation
593 (error-based) tasks. Studies using fMRI in healthy adults, and neural recordings or electrical
594 stimulation in pre-surgical patients, have provided evidence that the entorhinal cortex supports
595 the encoding of goal direction and distance, relative locations, and the clockwise or
596 counterclockwise direction of routes (Jacobs et al., 2010, 2016; Miller et al., 2013, 2015; Chadwick
597 et al., 2015; Goyal et al., 2018; Qasim et al., 2019). While our motor learning tasks did not involve
598 navigation in VR, the encoding of goal directions (in the visuomotor rotation task) and trajectories
599 to the goal (in the curve drawing task) were critical to learning. If the entorhinal cortex is important
600 for representing such spatial information, then its size may predict the ability to perform tasks —
601 perceptual and motor — that recruit such representations. Studies investigating the relation
602 between neuroanatomy and performance have associated greater gray matter volume in the
603 entorhinal cortex with better scene recognition (Whiteman et al., 2016), spatial memory (Hartley
604 and Harlow, 2012), navigation to memorized object locations in VR (Sherrill et al., 2018), as well
605 as the lifetime amount of video gaming (Kühn and Gallinat, 2014). Here, we extend these general
606 observations to include the previously unexplored domain of motor learning, showing an
607 association between right entorhinal volume and overall performance in error-based and reward-
608 based learning tasks. Given that motor learning has a strong visual-spatial component
609 (particularly so in our tasks), we find it noteworthy that it is the right, and not left, entorhinal cortex
610 that is associated with the processing and integration of visual-spatial information (Dalton et al.,
611 2016).

Author contributions

Conceptualization and methodology AJdB, JP, JPG, JRF; investigation AJdB; software AJdB; formal analysis AJdB, JP, MRR; visualization AJdB, JPG, MRR; writing - original draft AJdB, JPG; writing - review and editing AJdB, JP, JPG, JRF, MRR; supervision AJdB, JP, JPG; project administration AJdB, JP, JPG; resources JP, JPG, JRF; funding acquisition JP, JPG, JRF.

Acknowledgements

This work was supported by operating grants from the Canadian Institutes of Health Research (CIHR) awarded to J.R.F. and J.P.G. (MOP126158). J.P.G. and J.P. were supported by Natural Sciences and Engineering Research Council (NSERC) Discovery Grants, as well as funding from the Canadian Foundation for Innovation. The authors thank Mohammed Albaghdadi, Olivia Broda, Sydney Dore, Kate McKenzie and Reem Toubache for help with data collection, and Martin York for technical support.

References

Aronov D, Nevers R, Tank DW (2017) Mapping of a non-spatial dimension by the hippocampal-entorhinal circuit. Nature 543:719–722.

Bellmund JLS, Deuker L, Schröder TN, Doeller CF (2016) Grid-cell representations in mental simulation. eLife 5 Available at: http://dx.doi.org/10.7554/elife.17089.

Bellmund JLS, Gärdenfors P, Moser EI, Doeller CF (2018) Navigating cognition: Spatial codes for human thinking. Science 362 Available at: http://dx.doi.org/10.1126/science.aat6766.

Bond KM, Taylor JA (2015) Flexible explicit but rigid implicit learning in a visuomotor adaptation task. Journal of Neurophysiology 113:3836–3849 Available at: http://dx.doi.org/10.1152/jn.00009.2015.

Bostan AC, Strick PL (2018) The basal ganglia and the cerebellum: nodes in an integrated network. Nat Rev Neurosci 19:338–350.

Cashaback JGA, McGregor HR, Mohatarem A, Gribble PL (2017) Dissociating error-based and reinforcement-based loss functions during sensorimotor learning. PLoS Comput Biol 13:e1005623.

Chadwick MJ, Bonnici HM, Maguire EA (2014) CA3 size predicts the precision of memory recall. Proc Natl Acad Sci U S A 111:10720–10725.

Chadwick MJ, Jolly AEJ, Amos DP, Hassabis D, Spiers HJ (2015) A goal direction signal in the human entorhinal/subicular region. Curr Biol 25:87–92.

Codol O, Holland PJ, Galea JM (2018) The relationship between reinforcement and explicit

644 control during visuomotor adaptation. Sci Rep 8:9121.

645 Constantinescu AO, O'Reilly JX, Behrens TEJ (2016) Organizing conceptual knowledge in
646 humans with a gridlike code. Science 352:1464–1468.

647 Cunningham HA (1989) Aiming error under transformed spatial mappings suggests a structure
648 for visual-motor maps. J Exp Psychol Hum Percept Perform 15:493–506.

649 Dalton MA, Hornberger M, Piguet O (2016) Material specific lateralization of medial temporal
650 lobe function: An fMRI investigation. Hum Brain Mapp 37:933–941.

651 Dam G, Kording K, Wei K (2013) Credit assignment during movement reinforcement learning.
652 PLoS One 8:e55352.

653 Daw ND, Doya K (2006) The computational neurobiology of learning and reward. Curr Opin
654 Neurobiol 16:199–204.

655 de Brouwer AJ, Albaghdadi M, Flanagan JR, Gallivan JP (2018) Using gaze behavior to
656 parcellate the explicit and implicit contributions to visuomotor learning. J Neurophysiol
657 120:1602–1615.

658 Della-Maggiore V, McIntosh AR (2005) Time course of changes in brain activity and functional
659 connectivity associated with long-term adaptation to a rotational transformation. J
660 Neurophysiol 93:2254–2262.

661 Doya K (1999) What are the computations of the cerebellum, the basal ganglia and the cerebral
662 cortex? Neural Netw 12:961–974.

663 Doya K (2000) Complementary roles of basal ganglia and cerebellum in learning and motor
664 control. Curr Opin Neurobiol 10:732–739.

665 Doyon J, Benali H (2005) Reorganization and plasticity in the adult brain during learning of
666 motor skills. Curr Opin Neurobiol 15:161–167.

667 Duncan K, Doll BB, Daw ND, Shohamy D (2018) More Than the Sum of Its Parts: A Role for the
668 Hippocampus in Configural Reinforcement Learning. Neuron 98:645–657.e6.

669 Eichenbaum H, Cohen NJ (2014) Can we reconcile the declarative memory and spatial
670 navigation views on hippocampal function? Neuron 83:764–770.

671 Epstein RA, Patai EZ, Julian JB, Spiers HJ (2017) The cognitive map in humans: spatial
672 navigation and beyond. Nat Neurosci 20:1504–1513.

673 Fernandez-Ruiz J, Wong W, Armstrong IT, Flanagan JR (2011) Relation between reaction time
674 and reach errors during visuomotor adaptation. Behav Brain Res 219:8–14.

675 Fischl B, Salat DH, Busa E, Albert M, Dieterich M, Haselgrove C, van der Kouwe A, Killiany R,
676 Kennedy D, Klaveness S, Montillo A, Makris N, Rosen B, Dale AM (2002) Whole brain
677 segmentation: automated labeling of neuroanatomical structures in the human brain.
678 Neuron 33:341–355.

679 Fischl B, van der Kouwe A, Destrieux C, Halgren E, Ségonne F, Salat DH, Busa E, Seidman LJ,
680 Goldstein J, Kennedy D, Caviness V, Makris N, Rosen B, Dale AM (2004) Automatically

parcellating the human cerebral cortex. Cereb Cortex 14:11–22.

Galea JM, Mallia E, Rothwell J, Diedrichsen J (2015) The dissociable effects of punishment and reward on motor learning. Nat Neurosci 18:597–602.

Garvert MM, Dolan RJ, Behrens TE (2017) A map of abstract relational knowledge in the human hippocampal-entorhinal cortex. Elife 6 Available at: http://dx.doi.org/10.7554/eLife.17086.

Gershman SJ, Daw ND (2017) Reinforcement Learning and Episodic Memory in Humans and Animals: An Integrative Framework. Annu Rev Psychol 68:101–128.

Goyal A et al. (2018) Electrical Stimulation in Hippocampus and Entorhinal Cortex Impairs Spatial and Temporal Memory. J Neurosci 38:4471–4481.

Hafting T, Fyhn M, Molden S, Moser M-B, Moser EI (2005) Microstructure of a spatial map in the entorhinal cortex. Nature 436:801–806.

Haith AM, Huberdeau DM, Krakauer JW (2015) The influence of movement preparation time on the expression of visuomotor learning and savings. J Neurosci 35:5109–5117.

Hartley T, Harlow R (2012) An association between human hippocampal volume and topographical memory in healthy young adults. Front Hum Neurosci 6:338.

Heffley W, Song EY, Xu Z, Taylor BN, Hughes MA, McKinney A, Joshua M, Hull C (2018) Coordinated cerebellar climbing fiber activity signals learned sensorimotor predictions. Nat Neurosci 21:1431–1441.

Holland P, Codol O, Galea JM (2018) Contribution of explicit processes to reinforcement-based motor learning. J Neurophysiol 119:2241–2255.

Horner AJ, Bisby JA, Zotow E, Bush D, Burgess N (2016) Grid-like Processing of Imagined Navigation. Curr Biol 26:842–847.

Ito M, Doya K (2011) Multiple representations and algorithms for reinforcement learning in the cortico-basal ganglia circuit. Curr Opin Neurobiol 21:368–373.

Izawa J, Shadmehr R (2011) Learning from sensory and reward prediction errors during motor adaptation. PLoS Comput Biol 7:e1002012.

Jacobs J et al. (2016) Direct Electrical Stimulation of the Human Entorhinal Region and Hippocampus Impairs Memory. Neuron 92:983–990.

Jacobs J, Kahana MJ, Ekstrom AD, Mollison MV, Fried I (2010) A sense of direction in human entorhinal cortex. Proc Natl Acad Sci U S A 107:6487–6492.

Julian JB, Keinath AT, Frazzetta G, Epstein RA (2018) Human entorhinal cortex represents visual space using a boundary-anchored grid. Nat Neurosci 21:191–194.

Keisler A, Shadmehr R (2010) A shared resource between declarative memory and motor memory. J Neurosci 30:14817–14823.

Killian NJ, Jutras MJ, Buffalo EA (2012) A map of visual space in the primate entorhinal cortex. Nature 491:761–764.

717 Killian NJ, Potter SM, Buffalo EA (2015) Saccade direction encoding in the primate entorhinal
718 cortex during visual exploration. Proc Natl Acad Sci U S A 112:15743–15748.

719 Kostadinov D, Beau M, Blanco-Pozo M, Häusser M (2019) Predictive and reactive reward
720 signals conveyed by climbing fiber inputs to cerebellar Purkinje cells. Nat Neurosci 22:950–
721 962.

722 Krakauer JW, Ghez C, Ghilardi MF (2005) Adaptation to visuomotor transformations:
723 consolidation, interference, and forgetting. J Neurosci 25:473–478.

724 Kühn S, Gallinat J (2014) Amount of lifetime video gaming is positively associated with
725 entorhinal, hippocampal and occipital volume. Mol Psychiatry 19:842–847.

726 Lalazar H, Vaadia E (2008) Neural basis of sensorimotor learning: modifying internal models.
727 Curr Opin Neurobiol 18:573–581.

728 Larry N, Yarkoni M, Lixenberg A, Joshua M (2019) Cerebellar climbing fibers encode expected
729 reward size. Elife 8 Available at: http://dx.doi.org/10.7554/eLife.46870.

730 Maguire EA, Gadian DG, Johnsrude IS, Good CD, Ashburner J, Frackowiak RS, Frith CD
731 (2000) Navigation-related structural change in the hippocampi of taxi drivers. Proc Natl
732 Acad Sci U S A 97:4398–4403.

733 Makino H, Hwang EJ, Hedrick NG, Komiyama T (2016) Circuit Mechanisms of Sensorimotor
734 Learning. Neuron 92:705–721.

735 Mazzoni P, Krakauer JW (2006) An implicit plan overrides an explicit strategy during visuomotor
736 adaptation. J Neurosci 26:3642–3645.

737 Miller JF, Fried I, Suthana N, Jacobs J (2015) Repeating Spatial Activations in Human
738 Entorhinal Cortex. Current Biology 25:1080–1085 Available at:
739 http://dx.doi.org/10.1016/j.cub.2015.02.045.

740 Miller JF, Neufang M, Solway A, Brandt A, Trippel M, Mader I, Hefft S, Merkow M, Polyn SM,
741 Jacobs J, Kahana MJ, Schulze-Bonhage A (2013) Neural activity in human hippocampal
742 formation reveals the spatial context of retrieved memories. Science 342:1111–1114.

743 Nau M, Navarro Schröder T, Bellmund JLS, Doeller CF (2018) Hexadirectional coding of visual
744 space in human entorhinal cortex. Nat Neurosci 21:188–190.

745 Nikooyan AA, Ahmed AA (2015) Reward feedback accelerates motor learning. J Neurophysiol
746 113:633–646.

747 O'Keefe J, Dostrovsky J (1971) The hippocampus as a spatial map. Preliminary evidence from
748 unit activity in the freely-moving rat. Brain Research 34:171–175.

749 O'Keefe J, Nadel L (1978) The hippocampus as a cognitive map. Oxford University Press, USA.

750 Qasim SE, Miller J, Inman CS, Gross RE, Willie JT, Lega B, Lin J-J, Sharan A, Wu C, Sperling
751 MR, Sheth SA, McKhann GM, Smith EH, Schevon C, Stein JM, Jacobs J (2019) Memory
752 retrieval modulates spatial tuning of single neurons in the human entorhinal cortex. Nat
753 Neurosci 22:2078–2086.

754 Redding GM, Wallace B (1993) Adaptive coordination and alignment of eye and hand. J Mot
755 Behav 25:75–88.

756 Rodrigue KM, Raz N (2004) Shrinkage of the entorhinal cortex over five years predicts memory
757 performance in healthy adults. J Neurosci 24:956–963.

758 Romero JE, Coupé P, Manjón JV (2017) HIPS: A new hippocampus subfield segmentation
759 method. Neuroimage 163:286–295.

760 Schiller D, Eichenbaum H, Buffalo EA, Davachi L, Foster DJ, Leutgeb S, Ranganath C (2015)
761 Memory and Space: Towards an Understanding of the Cognitive Map. J Neurosci
762 35:13904–13911.

763 Seidler RD, Bo J, Anguera JA (2012) Neurocognitive contributions to motor skill learning: the
764 role of working memory. J Mot Behav 44:445–453.

765 Shadmehr R, Holcomb HH (1997) Neural correlates of motor memory consolidation. Science
766 277:821–825.

767 Shadmehr R, Krakauer JW (2008) A computational neuroanatomy for motor control. Exp Brain
768 Res 185:359–381.

769 Sherrill KR, Chrastil ER, Aselcioglu I, Hasselmo ME, Stern CE (2018) Structural Differences in
770 Hippocampal and Entorhinal Gray Matter Volume Support Individual Differences in First
771 Person Navigational Ability. Neuroscience 380:123–131.

772 Shmuelof L, Huang VS, Haith AM, Delnicki RJ, Mazzoni P, Krakauer JW (2012) Overcoming
773 motor “forgetting” through reinforcement of learned actions. J Neurosci 32:14617–14621.

774 Smith MA, Shadmehr R (2005) Intact ability to learn internal models of arm dynamics in
775 Huntington’s disease but not cerebellar degeneration. J Neurophysiol 93:2809–2821.

776 Sotiropoulos SN, Jbabdi S, Xu J, Andersson JL, Moeller S, Auerbach EJ, Glasser MF,
777 Hernandez M, Sapiro G, Jenkinson M, Feinberg DA, Yacoub E, Lenglet C, Van Essen DC,
778 Ugurbil K, Behrens TEJ, WU-Minn HCP Consortium (2013) Advances in diffusion MRI
779 acquisition and processing in the Human Connectome Project. Neuroimage 80:125–143.

780 Sutton RS, Barto AG (2018) Reinforcement Learning: An Introduction. A Bradford Book.

781 Tavares RM, Mendelsohn A, Grossman Y, Williams CH, Shapiro M, Trope Y, Schiller D (2015)
782 A Map for Social Navigation in the Human Brain. Neuron 87:231–243.

783 Taylor JA, Ivry RB (2011) Flexible cognitive strategies during motor learning. PLoS Comput Biol
784 7:e1001096.

785 Taylor JA, Ivry RB (2014) Cerebellar and prefrontal cortex contributions to adaptation,
786 strategies, and reinforcement learning. Prog Brain Res 210:217–253.

787 Taylor JA, Krakauer JW, Ivry RB (2014) Explicit and implicit contributions to learning in a
788 sensorimotor adaptation task. J Neurosci 34:3023–3032.

789 Tolman EC (1948) Cognitive maps in rats and men. Psychol Rev 55:189–208.

790 Tseng Y-W, Diedrichsen J, Krakauer JW, Shadmehr R, Bastian AJ (2007) Sensory prediction
791 errors drive cerebellum-dependent adaptation of reaching. J Neurophysiol 98:54–62.

792 Wagner MJ, Kim TH, Savall J, Schnitzer MJ, Luo L (2017) Cerebellar granule cells encode the
793 expectation of reward. Nature 544:96–100.

794 Whiteman AS, Young DE, Budson AE, Stern CE, Schon K (2016) Entorhinal volume, aerobic
795 fitness, and recognition memory in healthy young adults: A voxel-based morphometry
796 study. Neuroimage 126:229–238.

797 Wilming N, König P, König S, Buffalo EA (2018) Entorhinal cortex receptive fields are modulated
798 by spatial attention, even without movement. Elife 7 Available at:
799 http://dx.doi.org/10.7554/eLife.31745.